PHYSICAL REVIEW D VOLUME 19, NUMBER 3 1 FEBRUARY 1979

# Production of large-transverse-momentum protons

C. O. Escobar*
*Department of Applied Mathematics and Theoretical Physics, University of Cambridge, England*
(Received 17 May 1978)

We discuss in this paper two parton models for the production of large-$p_T$ protons. One is the multiple-scattering model of Landshoff, Polkinghorne, and Scott and the other one is the so-called leading-particle model. Several aspects of these models are discussed such as single-particle spectra, event structure, production on nuclear targets, and proton production from pion beams.

## I. INTRODUCTION

From the experiments of the Chicago-Princeton (CP)[1,2] and the British-Scandinavian (BS)[3] groups, it is known that there is a substantial production of baryons with large transverse momentum. The presence of these large-$p_T$ baryons is a challenge to the present models of large-$p_T$ production as it is difficult to find a natural mechanism for producing baryons at large $p_T$. This is particularly so for models in which the large-$p_T$ particle comes from the fragmentation of a quark,[4] since quarks do not frequently fragment into baryons (as we know from $e^+e^-$ and leptoproduction data) and what is more, the $p_T$ dependence of the proton cross section is given by $p_T^{-12}$ instead of the, by now familiar, $p_T^{-8}$ behavior exhibited by mesons.

An additional problem for those trying to build up a picture of large-$p_T$ baryons is the present experimental uncertainties. Unlike meson production, where a good agreement is found between different experimental groups,[5] in the case of baryon production there is a disagreement between the CP and the BS data in the kinematical region common to both experiments. The CP data are generally 20% below BS data for protons and up to 50% below for antiprotons. A particular example of these difficulties is the still unresolved puzzle of a $\bar{p}/p$ ratio near 1, found by BS at $p_T \approx 1.6$ GeV/$c$.

A further difficulty is that the CP group has two sets of data, one of which is taken with nuclear targets[1] and a second, more recent one, using a hydrogen target.[2] For their first set the CP group presented their results in the form

$$E\frac{d\sigma}{d^3p} \sim \frac{A^{\alpha(p_T)}}{p_T^{\,n}} f(x_T, \theta) \tag{1}$$

($x_T = 2p_T/\sqrt{s}$, $\theta$ is the center-of-mass scattering angle, and $A$ is the atomic number of the nuclear target) and found that the power $n$ had an $x_T$ dependence, approaching $n = 14$ for protons at large $x_T$ ($x_T \approx 0.6$). This behavior is, however, not seen in their experiments with a hydrogen target[2] where $n$ is fairly constant with $x_T$ and has the value $n \approx 12$ for protons.

Another puzzling result in experiments done with nuclear targets is the atomic-number dependence of the cross sections. As shown in (1), the CP group parametrizes this dependence as $A^{\alpha(p_T)}$ and finds[1,6] that at large $p_T$ ($p_T > 4$ GeV/$c$), $\alpha(p_T)$ has a value 1.1 for mesons and 1.3 for baryons, well beyond the $A^{2/3}$ dependence of low-$p_T$ reactions. In hard-scattering models a dependence such as $A^1$ is natural, due to the cancellations of initial and final state interactions.[7] It is, however, more difficult to understand $\alpha(p_T) > 1$, and this result seems to indicate that multiple scatterings, of one sort or the other, are occurring inside the nucleus therefore enhancing the cross sections.[8] It remains to be explained why the $A$ dependence for baryons is even more pronounced.

Before describing in detail the two models we shall consider in this paper, we must answer the question: What can be considered as a large $p_T$ for a baryon? It is known that for meson production one enters a new dynamical region when $p_T$ is greater than perhaps as little as 1 GeV/$c$. For protons, however, it seems that the new region is not reached until $p_T$ is at least of order 3 GeV/$c$. That this is so can be seen from the fact that $p$ and $\bar{p}$ cross sections fall off at small $p_T$ less steeply than the pion cross section and therefore at $p_T \approx 1$ GeV/$c$ there could be significant contributions coming from the tail of the low-$p_T$ mechanisms. This is in itself a problem, as a quick look at the experimental data shows that there are not many points for $p_T > 3$ GeV/$c$, especially in the CERN ISR experiments. We do not consider it reasonable to go below $p_T = 3$ GeV/$c$ when comparing theory with experiment.

The two models we describe in this paper have long been considered as serious candidates for explaining large-$p_T$ baryon production. The multiple-scattering model[8] is based on the mechanism considered by Landshoff in his discussion of wide-angle exclusive scattering.[9] It has some nice features such as a nonvanishing behavior at the

 

edge of phase space ($x_T \to \sin\theta$) and a natural explanation for the $A$ dependence of the cross section. It has a very distinct signature in the event structure on the away side. One of its apparent difficulties is that is predicts a $p_T^{-14}$ behavior which is not seen experimentally in the present $p_T$ range.

The other model considered in this paper is the leading-particle model[10] in which one of the incident protons is scattered at a wide angle from a quark belonging to the other proton. This model has been often mentioned[10,11] as a possible explanation for large-$p_T$ protons and it is worth considering it in detail. It has the advantage that a $p_T^{-12}$ behavior is expected if we follow the dimensional-counting rules;[12] however, it seems to have difficulties in explaining the $x_T$ dependence of the data as well as the structure of the away-side distributions, about which there is not much experimental information.

In this paper we show that by allowing the production of jets carrying baryon number in the leading-particle model, we can improve both the $x_T$ dependence and the away-side distribution.

We explore this model in detail and propose tests which could distinguish it from other models of large-$p_T$ protons. We come to the conclusion that the leading-particle model looks more promising than the multiple-scattering model when compared with the data.

We finally remark that no attempt is made here to explain $\bar{p}$ production. It seems that antiprotons are produced by a mechanism very different from those discussed in this paper as the CP data[2] indicate that the $\bar{p}$ spectrum falls of approximately like $p_T^{-8}$.

The paper is organized as follows. In the next section we discuss the multiple-scattering model. In Sec. III we consider the leading-particle model, while Sec. IV contains predictions and further tests of the leading-particle model.

## II. THE MULTIPLE-SCATTERING MODEL

### A. Introduction

We briefly review here the main results of the LPS paper[8] on the multiple-scattering quark-parton model.

This model, shown in Fig. 1, is based on the multiple scattering between constituents of the two colliding particles. In the case of proton production in proton-proton collisions, the constituents are valence quarks and each quark from one of the protons scatters on a quark from the other proton. The three outgoing wide-angle scattered quarks combine in order to form the large-$p_T$ proton. In order to do so, these three outgoing quarks must be aligned and this condition puts severe restrictions on the phase space available for the participants in the hard scatterings. When the central scatterings are scale-free, it is this limitation on the phase space which is responsible for the energy dependence of the cross section. Notice that the three away-side quarks are not forced to be aligned and that in general their combined invariant mass is large.

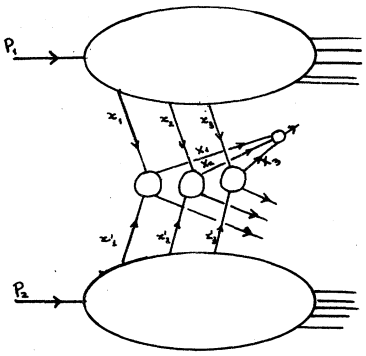

FIG. 1. The multiple-scattering mechanism for the production of large-$p_T$ protons.

With scale-free scattering for the hard collisions between the quarks, LPS found that the cross section is given by

$$E\frac{d\sigma}{d^3p} \sim \frac{1}{p_T^{14}} f(x_T, \theta). \tag{2}$$

The mechanism of Fig. 1 is a generalization to the inclusive case of the Landshoff diagram for wide-angle exclusive scattering[9] shown in Fig. 2. We can connect the two processes by arguments based on the exclusive-inclusive correspondence[13] and show that Fig. 1 does not vanish when we ap-

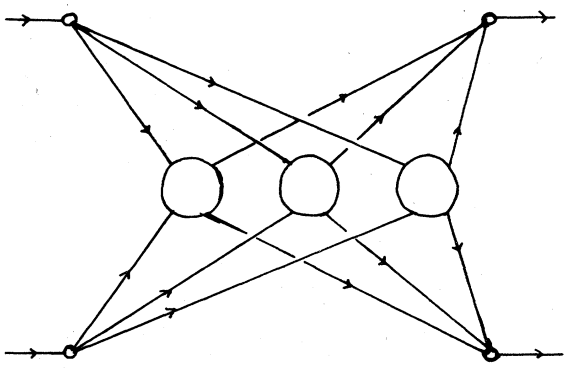

FIG. 2. The multiple-scattering mechanism for the wide-angle elastic scattering $pp \to pp$.

proach the edge of phase space, that is, when $x_T \to \sin\theta$. In this limit it is easy to see[8] that the surviving contribution comes from a configuration in which all of the momentum of the incident protons is carried by their three valence quarks.

As shown by LPS, the multiple-scattering model with scale-free central scatterings gives a cross section of the form

$$E\frac{d\sigma}{d^3p} \sim \frac{1}{p_T^{\,2}s^6}\int dx_1dx_2dx_3dx_1'dx_2'dx_3'dX_1dX_2dX_3T(x_1,x_2,x_3)T(x_1',x_2',x_3')G(X_1,X_2,X_3)$$
$$\times\,\delta\Big(1-\sum_{i=1}^{3}X_i\Big)\prod_{i=1}^{3}\Big[|A(x_i,x_i',X_i)|^2\delta\Big(\frac{x_ix_i'}{x_i\tan(\theta/2)+x_i'\cot(\theta/2)}-\frac{x_T}{2}X_i\Big)\Big],$$

where $T(x_1,x_2,x_3)$ is the probability of finding simultaneously in a nucleon three quarks carrying fractional momenta $x_1$, $x_2$, and $x_3$. $G(X_1,X_2,X_3)$ is the same distribution but for a proton which is in a configuration where all of its momentum is carried by the three valence quarks, hence the $\delta(1-\sum_{i=1}^{3}X_i)$. $A(x_i,x_i',X_i)$ is the scattering amplitude for the $i$th central collision for which we have the following invariants:

$$\begin{aligned} s_i &= x_ix_i's, \\ t_i &= -x_iX_i\frac{x_T}{2}\tan\frac{\theta}{2}s, \\ u_i &= -x_i'X_i\frac{x_T}{2}\cot\frac{\theta}{2}s. \end{aligned} \tag{4}$$

It is important to notice that in writing (3), it has been assumed that the transverse momentum of the quarks within each proton is very small, thus allowing an integration over all transverse variables, leaving only the longitudinal ones ($x_i, x_i'$, and $X_i$) to be integrated.

While in our actual calculations we always use scale-free scattering, it is appropriate to comment here on subasymptotic effects that may occur if we are not at a high enough $p_T$. These can be seen as follows. In the $q$-$q$ center-of-mass system and at $\theta=\pi/2$, $x_i=x_i'=x_TX_i$. Now $X_i$ is on average $\frac{1}{3}$ as we expect that $G(X_1,X_2,X_3)$ is peaked at $X_i=\frac{1}{3}$. We see then that in this situation

$$\begin{aligned} s_i &= \tfrac{4}{9}p_T^{\,2}, \\ t_i &= -\tfrac{2}{9}p_T^{\,2}, \end{aligned} \tag{5}$$

so that in the multiple-scattering case the invariants are much lower than in the situation where we have only one hard scattering ($\hat{s}\approx 4p_T^{\,2}$, $\hat{t}\approx -2p_T^{\,2}$).

If $p_T \geq 1$ GeV/$c$ marks the onset of the high-$p_T$ region for mesons (well described by single-scattering mechanisms) then we can see from (5) that we should have $p_T \geq 3$ GeV/$c$ in order to have collisions with the same $\hat{s}$ and $\hat{t}$ as in the single-scattering case. Below $p_T=3$ GeV/$c$ we would have to allow for modifications in the central scatterings which could then mask the $p_T^{-14}$ behavior. As there are many uncertainties on how to make such modifications, we prefer to apply the model to the very large-$p_T$ region ($p_T > 4.5$ GeV/$c$) where at least the CP collaboration has some data.

In order to estimate quantitatively the contribution of the multiple-scattering process we have to know the three-quark distribution function $T(x_1,x_2,x_3)$ and its disconnected piece $G(x_1,x_2,x_3)$ which will be discussed next.

### B. The three-quark distribution function

Even though the three-quark distribution is not easily accessible to experimental investigation or to theoretical insight, it is possible to make reasonable guesses about its behavior by using the knowledge we have from the single-quark distribution as measured in deep-inelastic leptoproduction.

We write the distribution function $T(x_1,x_2,x_3)$ as a sum of two terms

$$T(x_1,x_2,x_3)=G(x_1,x_2,x_3)\delta\Big(1-\sum_{i=1}^{3}X_i\Big) + F(x_1,x_2,x_3), \tag{6}$$

where, as mentioned before, $G(x_1,x_2,x_3)$ is the distribution function for the three valence quarks when they carry all the momentum of the proton and $F(x_1,x_2,x_3)$ is the probability of finding three valence quarks with longitudinal fractions $x_1, x_2$, and $x_3$ in a configuration in which the proton is more than just three valence quarks having in addition to them gluons and sea quarks.

We can learn something about $G$ by studying the behavior of the single-valence quark distribution

$q(x)$ as $x$ approaches one. In this limit all the momentum of the proton is carried by the valence quark and $q(x)$ is derived entirely from $G$.

As $q(x)$ is the probability of finding a valence quark with longitudinal fraction $x$, it is not difficult to see that the following relation holds:

$$q(x) \underset{x\to 1}{=} \int_s G(x_1 x_2, x_3)\delta(1-x-x_2-x_3)dx_2 dx_3, \quad (7)$$

where the region of integration $s$ is determined by

$$x+x_2+x_3=1, \quad 1 \geq x_i \geq 0 \quad (i=2,3).$$

If we assume that for large $x$, $q(x)$ behaves like

$$q(x) \underset{x\to 1}{\simeq} 3.4(1-x)^4, \quad (8)$$

as suggested by a recent fit[14] to the nucleon structure functions, then it is easy to see that $G(x_1, x_2, x_3)$, chosen for simplicity to be of the form

$$G(x_1, x_2, x_3) = 3(1-x_1)^3(1-x_2)^3(1-x_3)^3, \quad (9)$$

does give the required behavior for $q(x)$ as $x$ nears one.

We stress again that the above form for $G$ is chosen mainly for simplicity and that it sufficiently serves our purposes in this paper.

With respect to the other piece of $T$, $F(x_1, x_2, x_3)$, we require it to vanish as $(x_1+x_2+x_3)$ approaches one and that it should do so sufficiently fast in order to guarantee that its contribution to $q(x)$ is less important at $x \approx 1$ than that coming from $G$ [(7) and (8)].

For these reasons and again for the sake of simplicity we choose

$$F(x_1, x_2, x_3) = a(1-x_1-x_2-x_3)^3. \quad (10)$$

It is clear that $F$ contributes to $q(x)$,

$$q(x) = \int_s F(x, x_2, x_3)dx_2 dx_3, \quad (11)$$

where the domain $S$ is given by $x+x_2+x_3 \leq 1$, $x_i \geq 0$. Using (10) this will give $q(x)$ behaving like $(1-x)^5$ as $x \to 1$, which, as desired, vanishes faster than the contribution from $G$. The normalization constant $a$ can be determined from the overall normalization of $T(x_1, x_2, x_3)$,

$$\int T(x_1, x_2, x_3)dx_1 dx_2 dx_3 = 1. \quad (12)$$

Using (9) and (10) this will give a $\simeq 100$.

In the following we use the three-quark distribution,

$$T(x_1, x_2, x_3) = 3(1-x_2)^3(1-x_2)^3(1-x_3)^3\delta\left(1-\sum_{i=1}^{3}x_i\right) + 100(1-x_1-x_2-x_3)^3, \quad (13)$$

noticing that no distinction has been made between $u$ and $d$ quarks, which is why $T$ is symmetrical in $x_1$, $x_2$, and $x_3$.

The determination of the three-quark distribution function has also been investigated by Pokorski and Van Hove[15] in their model of nondiffractive hadronic collisions. Our approach differs from theirs in that we include the term $G(x_1, x_2, x_3)\delta(1-\sum_{i=1}^{3}x_i)$ which we believe is important, while they do not consider it at all. Also for our purposes, we do not need the more complicated distributions suggested by them.

### C. $pp \to p + X$

The final ingredient missing for the calculation of the inclusive cross section is the quark-quark hard-scattering cross section. Assuming the scattering to be scale-free and mediated by the exchange of an octet of colored vector gluons, we then have

$$\frac{d\sigma}{dt_i} = \frac{4\pi}{9}\alpha_s^2 \frac{s_i^2+u_i^2}{t_i^2}, \quad (14)$$

where $s_i$, $t_i$, and $u_i$ are given in (4) and $\alpha_s$ is the quark-gluon coupling constant, which according to estimates[16] from quantum chromodynamics is $\alpha_s \approx 0.3$. Notice that in (14) we have neglected interference terms which will not make a great difference to our results, given the roughness of our estimates.

With everything now determined it could seem that the overall normalization of the multiple-scattering mechanisms is fixed. However, we must remember that in order for the cross section to have the right dimension we need the tenth power of a mass scale which will determine the overall normalization of the cross section. If, as has been recently suggested by Landshoff and Polkinghorne[22] in their analysis of the multiple-scattering process in calorimeter-trigger experiments, this mass scale is the inverse proton radius, $\mu = R_p^{-1} \approx 140$ MeV, we find that the multiple-scattering cross section is so small that it could not be observed in the currently available energy and transverse-momentum range. On the other hand, if we allow the mass scale to be as large as 500 MeV then the multiple-scattering mechanism could still be seen at very large transverse momenta in present-day experiments.

This point is illustrated in Fig. 3 where we show the multiple-scattering cross section normalized with the choice $\mu = 500$ MeV and compared with the CP data at $\sqrt{s} = 27.4$ GeV. For transverse momenta larger than currently available ($p_T > 7$ GeV) we have extrapolated the experimental data according to

$$E\frac{d\sigma}{d^3p} = 230\frac{(1-x_T)^7}{p_T^{12}} \text{ (mb GeV}^{-2}\text{)}, \quad (15)$$

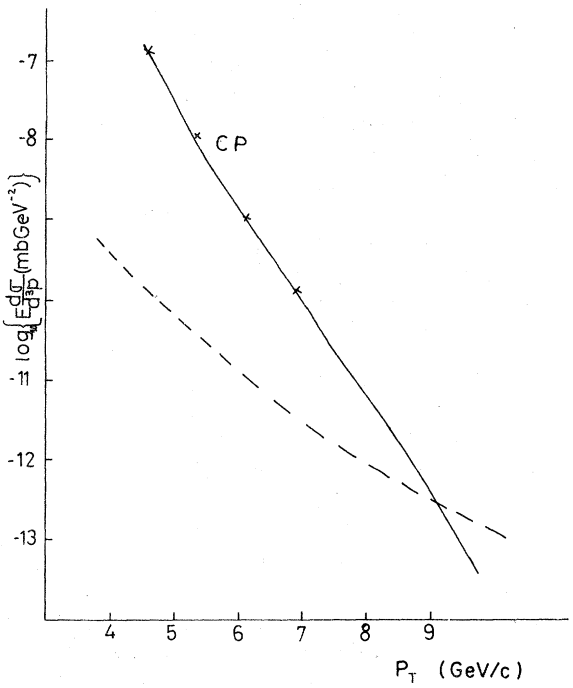


FIG. 3. Comparison between the multiple-scattering model and the CP data at $\sqrt{s}=27.4$ GeV (Ref. 2). At large $p_T$, beyond the experimental range currently covered by CP ($p_T>7$ GeV/$c$), the data have been extrapolated according to the fit (15).

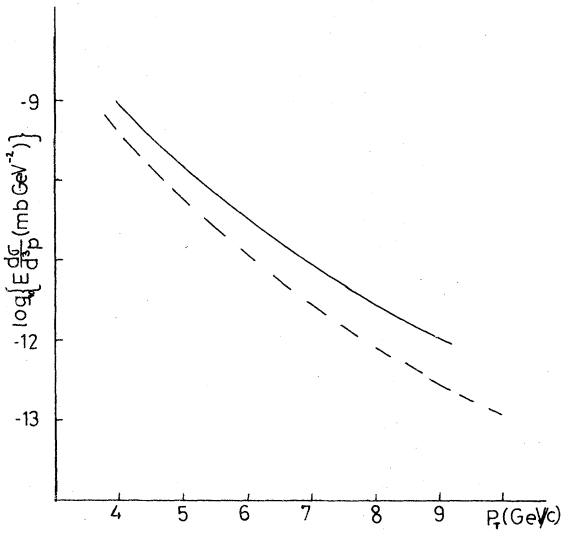


FIG. 4. The multiple-scattering cross section for $pp\to p+X$ at two CP energies, $\sqrt{s}=27.4$ GeV (dashed line) and $\sqrt{s}=23.7$ GeV (solid line).

which is a very reasonable fit for $x_T>0.4$.

For $p_T>9$ GeV the multiple-scattering mechanism dominates over the extrapolation of (15) because of its nonvanishing behavior as $x_T$ nears one and the fact that the cross section has the dependence $p_T^{-2}\,s^{-6}$ indicated in (3). These two factors are responsible for a less steep fall of the cross section with $p_T$, at fixed energy. On the other hand, as we have just seen, the magnitude of the cross section is small due to the energy behavior $s^{-6}$. Notice that as the central scatterings are scale-free they do not introduce any further $p_T$ dependence.

From these remarks we can conclude that the best place to look for the multiple-scattering contribution to the single-particle spectrum is at very large transverse momenta and not so large energies. As a matter of fact, unlike other large-$p_T$ models, the multiple-scattering model, with scale-free scatterings, gives a cross section which, at fixed $p_T$, decreases as the center-of-mass energy increases. This is shown in Fig. 4 where we compare our results at two CP energies. This energy behavior is a characteristic feature of the model.

To conclude this section we stress once again that the results of Figs. 3 and 4 were obtained by using a quite large mass scale, $\mu=500$ MeV. If we use a perhaps more realistic mass $\mu=140$ MeV, our results would be so small that they would escape experimental observation.

### D. Event structure

A study of the final states associated with a large-$p_T$ proton trigger would be most useful in helping to discriminate between the several models. In particular, the multiple-scattering model has a very striking event structure as pointed out by LPS. We here discuss only two aspects of this structure, the associated multiplicity on the away-side of the proton trigger and the $P_{\text{out}}$ distribution, the distribution of the momentum component on the away-side perpendicular to the beam-trigger plane (see Fig. 5).

The dependence of the associated multiplicity on the quantum numbers of the trigger is useful information for our understanding models of large-transverse-momentum production. The DILR collaboration[17] has data on the multiplicity associated with various types of triggers, including protons.

They fit their data according to the expression

$$\langle n_h\rangle(\phi,p_T,\sqrt{s}\,)=A_h(\phi)+B_h(\phi)p_T+C_h(\phi)\ln\frac{s}{s_0}, \tag{16}$$

where $\langle n_h\rangle$ is the average multiplicity associated with a trigger of type $h$, $\phi$ is the azimuthal angle

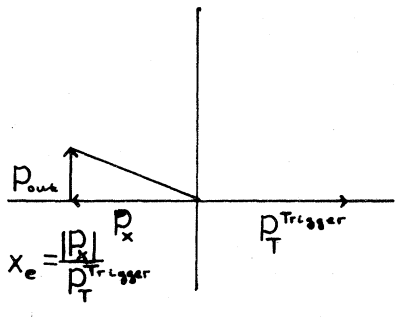


FIG. 5. The definition of $P_{\text{out}}$ and $x_e$.

($\phi = 0°$ is the same-side and $\phi = 180°$ the away-side), and $p_T$ is the trigger transverse momentum.

The most interesting term is the $p_T$-dependent one, namely $B_h(\phi)p_T$. Theoretically, we expect a logarithmic multiplicity,[18]

$$\langle n_h \rangle = a_h + b_h \ln P \tag{17}$$

reflecting the $dz/z$ spectrum of the fragmenting parton of momentum $P$.

Even though the DILR parametrization is linear in $p_T$, we can still compare the magnitude of the $p_T$ dependent terms with the theoretical expression (17), as in the $p_T$ range involved ($p_T \leq 5$ GeV/$c$) the deviations between a logarithmic dependence and a linear one are not very significant.

The data show that $B_p > B_{\pi^\pm}$ and $A_p > A_{\pi^\pm}$ but only slightly so. For instance, at $p_T = 3$ GeV/$c$ and $\sqrt{s} = 45$ GeV, it is found that on the away side $\langle n_p \rangle - \langle n_\pi \rangle = 0.25$.

According to LPS we would expect, in the multiple-scattering model, a far greater multiplicity on the away side. They argue that as in this mechanism the transverse momentum of the trigger is balanced by three quarks, the very fact that there are three of them will tend to increase the multiplicity as compared to that obtained in models with just one hard scattering, where the trigger is balanced by one jet (a quark or a meson depending on the model).

We want to show here that in order to see this effect we have to go to quite large $p_T$, beyond the DILR range. Our argument is as follows. In the case of a single-scattering mechanism, the away-side jet carries on average a momentum $p_T/\langle z \rangle$ where $\langle z \rangle$ is the average fraction of the momentum of the same-side jet which is carried by the trigger. Therefore, the away-side multiplicity is given by

$$\langle n_h \rangle = a_h + b_h \ln \frac{p_T}{\langle z \rangle}. \tag{18}$$

On the other hand, in the multiple-scattering model each away-side quark carries on average a momentum $p_T/3$ as there are three quarks balancing the trigger and where we have assumed, as throughout this paper, that the large-$p_T$ proton is produced alone [remember the condition $\delta(1 - \sum_{i=1}^{3} X_i)$ in Eq. (3)].

If we use, for definiteness and for the sake of comparison, the value $\langle z \rangle = 0.82$ for a pion trigger, obtained in a quark-quark scattering model,[4,11] we then have for the proton minus pion trigger multiplicity on the away-side

$$\langle n_p \rangle - \langle n_\pi \rangle = 2a + 3b \ln \frac{p_T}{3} - b \ln \frac{p_T}{0.82}. \tag{19}$$

Using $a = 0.09$ and $b = 1.5$, which approximately fits the data for pions,[11] we see that in order for the proton multiplicity to become greater than the pion, the trigger $p_T$ has to be quite large,

$$\langle n_p \rangle > \langle n_\pi \rangle \text{ for } p_T > 5.4 \text{ GeV}/c, \tag{20}$$

which is outside the DILR range. Of course, as $p_T$ increase beyond this value, the original argument given by LPS applies and the proton associated multiplicity becomes larger than the one associated with a pion trigger. Therefore it seems that the multiple-scattering contribution is not yet seen in the DILR data.

We now turn to a discussion of the $P_{\text{out}}$ distribution. The expectation in the multiple-scattering model is that it should be broader than it is for mechanisms involving a single scattering; the reason is that as we now have three quarks participating in the hard scatterings, this would enhance, through cumulative effects, the expected deviation from coplanarity due to the transverse momentum of quarks inside the hadrons.[8,19]

We here want to call attention to another aspect of this violation of coplanarity, namely the much larger $x_e$ dependence of $\langle P_{\text{out}} \rangle$ ($x_e$ is defined in Fig. 5) exhibited by the multiple-scattering model.

In the single quark-quark scattering case, the approximate $x_e$ dependence of $\langle P_{\text{out}} \rangle$ was given by Fox[11] as

$$\langle P_{\text{out}} \rangle = [\langle k_T \rangle_{h \to q}^2 x_e^2 + \tfrac{1}{2} \langle k_T \rangle_{q \to h}^2 (1 + x_e^2)]^{1/2}, \tag{21}$$

where $\langle k_T \rangle_{h \to q}$ is the mean internal transverse momentum of quarks in hadrons and $\langle k_T \rangle_{q \to h}$ that of hadrons coming from the fragmentation of a quark.

In the multiple-scattering case, provided at least one of the central scatterings has the transverse-momentum bias responsible for the validity of (21), we can apply the same expression with the reservation that now we must replace $x_e$ by

$$x_e' = \frac{|p_x|}{p_T/3} = 3x_e$$

as each away-side quark has on average a mo-

mentum $p_T/3$ and where we are assuming that the three away-side quarks fragment independently of each other. We must also remember that as we have for simplicity always considered the case in which the large-$p_T$ proton is produced alone, the last term in (21), $\frac{1}{2}\langle k_T\rangle_{q\to h}{}^2 x_e{}^2$ is now absent. With these precautions we obtain

$$\langle P_{\text{out}}\rangle = [\langle k_T\rangle_{h\to q}{}^2 9x_e{}^2 + \tfrac{1}{2}\langle k_T\rangle_{q\to h}{}^2]^{1/2}\ , \tag{22}$$

which, due to the factor 9, shows a very pronounced dependence on $x_e$. It should be remarked that large $x_e$ is presumably rather rare in the multiple-scattering process, as it is hard to find, given the above assumptions, a particle on the opposite side carrying $x_e > \frac{1}{3}$. Even so, the $x_e$ dependence obtained in (22) could be seen at small $x_e$ ($x_e < \frac{1}{3}$). This is shown in Fig. 6 where we have used $\langle k_T\rangle_{h\to q} = 500$ MeV/$c$ and $\langle k_T\rangle_{q\to h} = 300$ MeV/$c$ which are reasonable values according to the recent experimental findings of large internal transverse momentum for the partons.[19,20] As can be seen, large values of $\langle P_{\text{out}}\rangle$ are obtained, even for quite small values of $x_e$.

### E. Nuclear-target effects

We will briefly comment on the predictions of the multiple-scattering mechanism for the atomic-number dependence of the cross section which was mentioned in the Introduction.

It was shown by LPS that we obtain in this model

$$E\frac{d\sigma}{d^3p} \sim p_T{}^{-14}[Af_1(x_T,\theta) + A^{4/3}f_2(x_T,\theta) + A^{5/3}f_3(x_T,\theta)]. \tag{23}$$

The origin of the different terms is as follows. The first term occurs rather than $A^{2/3}$ seen at small $p_T$, because of the cancellations of initial- and final-state interactions.[7] The second and third terms follow from the possibility that the quarks in Fig. 1 come from different nucleons. In fact we might expect an $A^2$ and $A^3$ dependence, simply based on combinations, but as suggested by Mueller,[21] from a space-time view of the process, $A^{4/3}$ and $A^{5/3}$ terms are more reasonable.

The important features of (23) are that all three terms have the same $p_T$ dependence and that even though it is difficult to estimate quantitatively the magnitudes of $f_2$ and $f_3$, it is expected that $f_1 > f_2 > f_3$ as $f_2$ and $f_3$ involve scatterings between constituents coming from widely separated parts of the nucleus.

In order to avoid the difficult transition region from $\alpha \approx 0.8$ at low $p_T$ to $\alpha > 1$ at large $p_T$, we compare the multiple-scattering result (23) with experiment in the region where $\alpha(p_T)$ is approximately constant. As mentioned in the introduction, for $p_T > 4$ GeV/$c$ $\alpha$ is approximately constant and equal to 1.3 for protons. Defining the ratio

$$r(A) = \frac{\sigma(p + A \to p + X)}{\sigma(p + \mathrm{W} \to p + X)}, \tag{24}$$

that is, the cross section for proton production on a target with atomic number $A$ relative to tungsten ($A_{\mathrm{W}} = 184$), the CP group obtains $r(A) = (A/184)^{1.3}$ which gives a straight line in a log-log plot. We calculate $r(A)$ using (23) and find good agreement with the CP group for $f_2/f_1 = 0.3$ and $f_3/f_1 = 0.03$. This is shown in Fig. 7 where the solid line is the model prediction and the dashed line is the CP re-

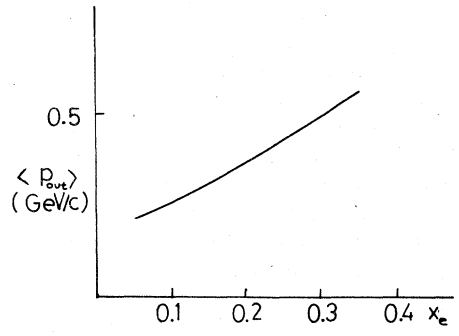


FIG. 6. The dependence of $\langle P_{\text{out}}\rangle$ on $x_e$. The curve is calculated using Eq. (22) with $\langle k_T\rangle_{q\to h} = 300$ MeV and $\langle k_T\rangle_{h\to q} = 500$ MeV.

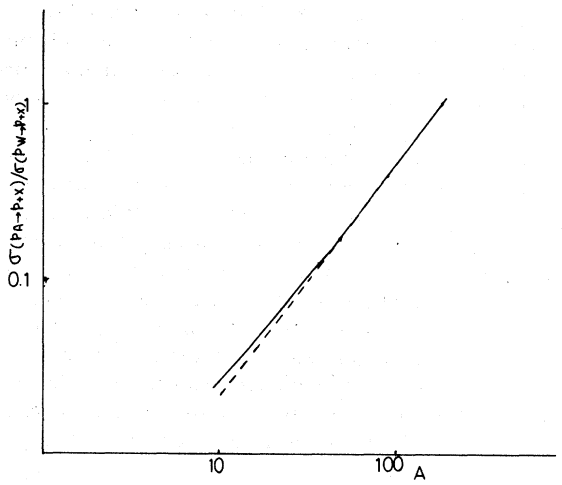


FIG. 7. The cross section for production of a large-$p_T$ proton on a target of atomic number $A$, relative to tungsten. The dashed line is the CP fit (Ref. 6) with $\alpha(p_T) = 1.3$ and the solid line is the multiple-scattering prediction.

sult. As can be seen our result deviates from the straight line for small atomic numbers ($A < 20$) which is perhaps not so surprising, as maybe multiple-scattering occurs only for heavy nuclei and not for light nuclei.

We notice that $f_2$ and $f_3$ come out rather large. However, as we are unable to compute their magnitudes, it is not yet clear if their large contribution poses a problem for the multiple-scattering process.

### F. Concluding remarks on the multiple-scattering model

We have seen that an actual computation of the multiple-scattering mechanism is clouded by many uncertainties, namely the fact that the three-quark distribution $T(x_1, x_2, x_3)$ is unknown, that subasymptotic effects are more important in this model than in other large-$p_T$ models, not to forget that the starting point of our calculations, Eq. (3), is an approximation which neglected the transverse momentum of the quarks inside the proton, an effect which is again likely to be more important here than in single-scattering models, where probably it is already not negligible.[19,20] We also have the already mentioned uncertainty in the normalization of the cross section (Sec. III C), where a smaller mass scale could rule out the chances of the multiple-scattering process from ever being seen in single-particle inclusive and exclusive[9] ($pp$ elastic) experiments in the present experimental range, even though it could still be observed in calorimeter-trigger experiments.[22]

As seen in Sec. II D the event structure of this model is remarkable and a study of it offers the best possibility of looking for this mechanism. Again the complicated kinematics of the multiple-scattering process did not allow us to make more than just semiquantitative and qualitative observations about this event structure.

With respect to the nuclear-target effects, the $A$ dependence predicted by this model is not in disagreement with the data for heavy nuclei, as discussed in the last Sec. II E, but an actual calculation remains to be done. The difficulties for such a calculation are now even greater as we have to solve, in addition to the above-mentioned problems, a difficult problem of nuclear physics, namely, how to compute the probabilities that a second and third nucleon, widely separated from each other, participate in the large-$p_T$ collision.

## III. THE LEADING-PARTICLE MODEL

### A. Description of the model

The leading-particle mechanism, shown in Fig. 8, is based on the high-energy, wide-angle scattering of a quark from one of the hadrons off the other hadron. Using the dimensional-counting rules[12] for the wide-angle quark-proton scattering, we obtain a cross section varying as $p_T^{-12}$. Of course, we still have to specify the angular dependence of the $q$-$P$ scattering amplitude, and it is one of our purposes in this paper to show how the experimental data can help us in choosing an adequate form for it.

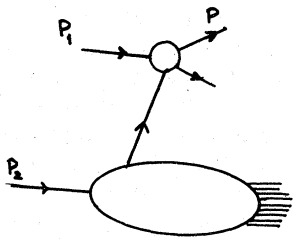


FIG. 8. The leading-particle mechanism for the production of a large-$p_T$ proton.

We remark that there is no need to be restricted to $qP \to qP$ elastic scattering, and it is in fact more realistic to allow for the production of baryon resonances or even a continuum with baryon quantum numbers (a superposition of multibody baryon resonances?). We represent this latter possibility by the quasi-two-body scattering $qP \to qB^*$ is an excited baryonic system which subsequently decays into a nucleon plus other particles, $B^* \to N + X$. This modification of the leading-particle model is a natural one and is in line with the recent findings of a jet structure in large-$p_T$ experiments.[23]

It is such a modified leading-particle mechanism that is considered in this paper.

We assume that the quark-proton scattering amplitude can be written in the simple form[10]

$$A(qP \to qB^*) \sim \gamma^\mu \gamma_u \hat{s}^{-3} \psi\left(\frac{-\hat{t}}{3}\right), \tag{25}$$

where the $S$ dependence is suggested by the dimensional-counting rules and the angular dependence has been simply factored out in the, as yet unknown, function $\psi$. The spin structure $\gamma^\mu \gamma_u$ is chosen as we have spin-$\frac{1}{2}$ quarks and protons and are assuming a spin-1 diquark core. We have verified that our results are not very sensitive to the assumed spin structure of $A$.

The invariants for the hard scattering are

$$\begin{aligned} \hat{s} &= x, s, \\ \hat{t} &= -\frac{x_2}{z} s, \\ \hat{u} &= -\frac{x x_1}{z} s, \end{aligned} \tag{26}$$

where

$$x_1=\frac{x_T}{2}\cot\frac{\theta}{2},\quad x_2=\frac{x_T}{2}\tan\frac{\theta}{2},$$

and $\theta$ is the center-of-mass scattering angle. In the above expressions $x$ is the fractional momentum carried by the quark and $z$ is the fraction of the jet's momentum taken by the large-$p_T$ proton.

Using (25) we obtain for the single-particle inclusive cross section

$$E\frac{d\sigma}{d^3p}=\frac{1}{s^6}\sum_q\int_{1-\epsilon}^1 dZ\,\frac{g_p(z)}{z}\,\frac{1+x_1^2/z^2}{1-x_1/z}F_{q/p}(x)\times\frac{1}{x^6}\,|\psi(1-x_1/z)|^2. \tag{27}$$

In (27), $F_{q/p}(x)$ are the quark distribution functions, measured in deep-inelastic leptoproduction experiments. $g_p(z)$ is the jet fragmentation function which gives the probability of finding, among the jet's fragments, a proton carrying a fraction $z$ of the jet's momentum.

The two-body scattering constraint ($s+t+u=0$) implies that

$$x=\frac{x_2}{z-x_1} \tag{28}$$

and the condition $x\leq 1$ gives $1>z>1-\epsilon$, where $\epsilon=1-x_1-x_2$. We sum in (27) over all quark flavors which contribute to the hard scattering. If we use a quark-interchange picture[24] for this scattering, shown in Fig. 9, where the wavy line is the diquark core, then only those quarks which are present in the valence component of the proton will contribute to the scattering, that is, only $u$ and $d$ quarks.

To proceed with the calculation of the invariant cross section we must know the quark distribution function $F_{q/p}(x)$, the jet fragmentation function $g_p(z)$, and the angular dependence of the $q$-$P$ scattering [the function $\psi(-\hat{t}/\hat{s})$].

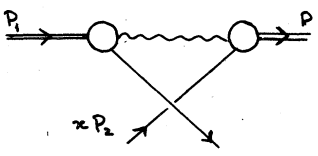


FIG. 9. A quark-interchange model for the $q$-$p$ scattering. The wavy line is a diquark core, the thick lines are the incoming and outgoing protons, and the interchanged particles are valence quarks.

### B. Quark distribution functions

We shall use for $F_{q/p}(x)$ a two-component fit which separates the valence ($V_{q/p}$) and the sea ($S_{q/p}$) contributions to $F_{q/p}$. We choose for $V$ and $S$ the fits suggested by Donnachie and Landshoff[14] which are shown in Table I, where their corresponding functions for a pion are also shown, which we will need later when calculating the beam ratio.

### C. The jet fragmentation function, $g_p(z)$

Unfortunately not much is experimentally known about the jet on the same side of a large-$p_T$ proton trigger. There is, however, evidence from the BFS collaboration[23] that such a jet exists and is strongly biased by the large-$p_T$ trigger. This can be better seen from their measurement of the momentum carried by charged particles moving along the trigger. As expected in a jet picture, they find that the extra momentum on the trigger side increases with the transverse momentum of the trigger and because the jet is biased by the trigger, this additional momentum is not very large ($\leq 0.2P_{\text{trigger}}$). In this respect the situation for protons is thus similar to that for pion triggers.[23]

An analysis by Ellis, Jacob, and Landshoff[25] showed that for meson triggers the same-side jet is well described if it contains, in addition to the multiparticle contribution, a single-particle term representing the possibility that the jet has only one particle, the trigger. We adopt this prescription and write for the same-side jet

$$g_p(z)=a_p\frac{(1-z)^m}{z}+b_p\delta(1-z), \tag{29}$$

with $b_p\ll a_p$ in order to ensure that the probability of finding a single particle in a freely fragmenting jet is small.[25] We will later find that $m=2$ gives a good description of the data, in particular the behavior of the single-particle cross section.

The function $g_h(z)$ satisfies the momentum sum rule

$$\sum_h\int_0^1 z g_h(z)dz=1, \tag{30}$$

where we sum over all hadrons $h$ produced by the jet. Neglecting the second term in (29), we get

$$\sum_h a_h=3. \tag{31}$$

It is difficult to estimate how much momentum is carried by neutral particles and by charged particles other than the proton. Notice that in the way we have defined $g_p(z)$, we could have production of a jet carrying the quantum numbers of a neutron (simply by a $u$-$d$ interchange in Fig. 9); we there-

TABLE I. Quark distribution functions used in this paper according to Ref. 14.

| | | | |
|---|---|---|---|
| $V_{q/p}$ | $x^{1/2}(1-x)^2$ | $x<0.2$ | $F_{u/p}+F_{d/p}=3V_{q/p}+2S_{q/p}$ |
| | $3.45x(1-x)^4$ | $x>0.2$ | |
| $S_{q/p}$ | $0.18[1-x^{1/2}(2-1.33x+04x^2)]$ | $x<0.2$ | |
| | $0.124(1-x)^5$ | $x>0.2$ | |
| $V_{q/\pi}$ | $0.65x^{1/2}(1-x)^{1/2}$ | $x<0.5$ | |
| | $1.3x(1-x)$ | $x>0.5$ | $F_{u/\pi^+}+F_{d/\pi^+}=V_{q/\pi}+2S_{q/\pi}$ |
| $S_{q/\pi}$ | $0.12\{1-0.65[\sin^{-1}x^{1/2}+x^{1/2}(1-x)]\}$ | $x<0.5$ | $F_{d/\pi^-}+F_{u/\pi^-}=V_{q/\pi}+2S_{q/\pi}$ |
| | $0.078(1-x)^2$ | $x>0.5$ | |

fore guess that $\frac{1}{3}$ of the momentum is carried by neutral particles and approximately $\frac{2}{3}$ is carried by the proton. This estimate gives

$$a_p=2. \tag{32}$$

The constant $b_p$ will be determined from an analysis of the single-particle cross section, and we will come back to this point later on. Ideally all the parameters of $g_p(Z)$ should be determined from a comparison with the experimental data on correlations. As such data are lacking for proton triggers we had to use the single-particle cross section to fix some of the parameters such as $m$ and $b_p$. Once the data are available there should be no problem in analyzing them with the model here described.

### D. Determination of the angular dependence, $\psi(-\frac{\hat{t}}{\hat{s}})$

The BS collaboration[3] found that for fixed $p_T$ the proton cross section is roughly constant in the range $40°\leq\theta_{cm}\leq 90°$. We compare these data with the leading-particle model for several choices of $\psi(-\hat{t}/\hat{s})$. Figure 10 shows the data and our results. All theoretical curves are normalized to agree at $\theta=90°$. With $\psi$ of the form

$$\left|\psi\left(\frac{-\hat{t}}{\hat{s}}\right)\right|^2=\left(1+\frac{\hat{t}}{\hat{s}}\right)^{-\alpha}=\left(\frac{-\hat{u}}{\hat{s}}\right)^{-\alpha}, \tag{33}$$

we find that $\alpha=6$ gives a fairly constant cross section in the interval $40°\leq\theta_{cm}\leq 90°$. $\alpha<4$ does not seem to be favored by the data as it gives a peak at forward angles. We remark that these results can be modified if we take into account the effects of the transverse-momentum spread in the jet fragmentation and the quark transverse momentum inside the proton, as it is known that these have the consequence of smoothing the forward peak in the angular distribution.[19,26] Anyway, it seems that $\alpha=6$ does give a good description of the data and in the following we use

$$\left|\psi\left(\frac{-\hat{t}}{\hat{s}}\right)\right|^2=\left(\frac{\hat{s}}{\hat{u}}\right)^6. \tag{34}$$

Such a strong $\hat{u}$ dependence is suggested by the quark-interchange mechanism of Fig. 9, with a spin-1 diquark core.

### E. Normalization

We normalize our cross section by comparing it with the CP data shown in Fig. 11. This allows us to determine the constant $b_p$ defined in (29) and an overall normalization constant $N$ which always comes in the combination $Na_p$ and $Nb_p$.

Our choice of normalization corresponds to

$$\frac{b_p}{a_p}=2.5\times 10^{-4}. \tag{35}$$

This choice for $b_p$ is dictated by the shape of the

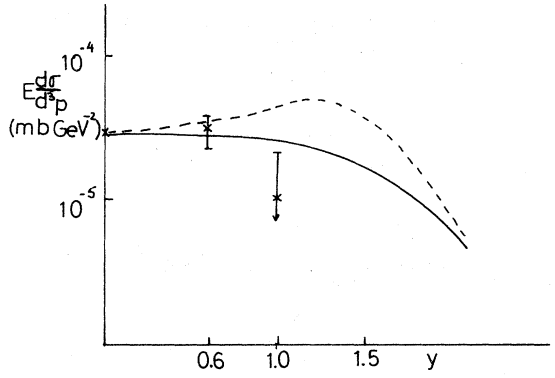


FIG. 10. The angular dependence of the $pp\to p+X$ cross section for two different choices of the $q$-$p$ amplitude: (a) $|\psi|^2=\hat{s}^6/u^6$ (solid line) and (b) $|\psi|^2=\hat{s}^4/\hat{u}^4$ (dashed line).

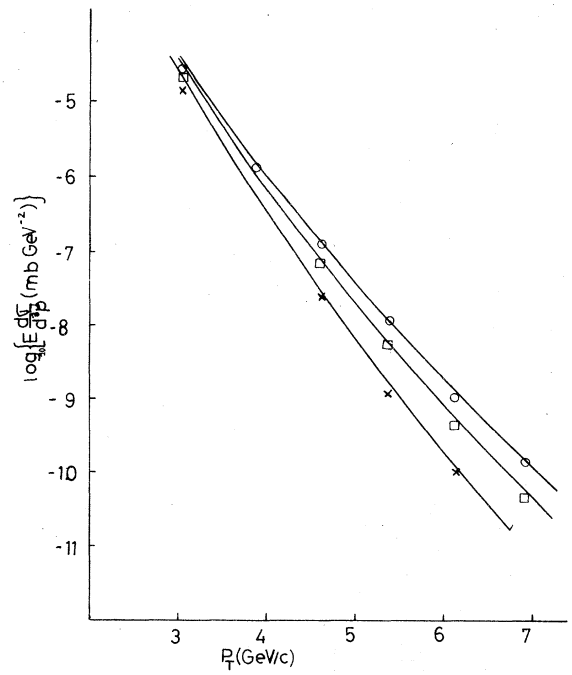


FIG. 11. The invariant cross section for $pp \to p + X$ in the leading-particle model, compared with the CP data (Ref. 2). Open circles $\sqrt{s} = 27.4$ GeV, open squares $\sqrt{s} = 23.7$ GeV, and crosses $\sqrt{s} = 19.4$ GeV.

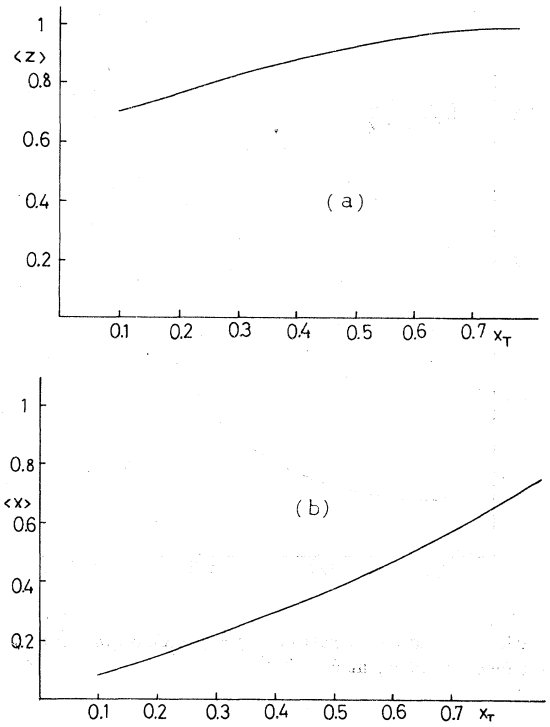


FIG. 12. (a) The average fraction of the momentum of the jet, which is taken by the large $p_T$ proton. (b) The average fraction of the momentum carried by the quark.

cross section in Fig. 11. A larger $b_p$ would make the calculated cross section become greater than the experimental one at large $p_T$ and a smaller $b_p$ would bring disagreement at small $p_T$. With $a_p = 2$, the overall normalization constant $N$ has the value

$$N = 10^3 \text{ mb GeV}^{10}. \tag{36}$$

The agreement with the data is very good, as can be seen from Fig. 11.

Figure 12 shows two quantities which will be of interest later on: $\langle z \rangle$ is the mean value of the fraction of the jet's momentum taken by the large-$p_T$ proton and $\langle x \rangle$ is the mean value of the longitudinal fraction $x$, carried by the quark. $\langle z \rangle$ will be needed when calculating the associated multiplicity on the away-side and $\langle x \rangle$ will help us to understand the results on the pion/proton beam ratio.

## IV. PREDICTIONS AND FURTHER TESTS OF THE MODEL

### A. The $\pi/p$ beam ratio

Experiments at large $p_T$ using different types of beam particles are one of the best tests of large-$p_T$ models.[11,19] In the leading-particle model, the process $\pi p \to p + X$ has the same $p_T$ dependence as $pp \to p + X$, namely $p_T^{-12}$, so that the ratio $\sigma(\pi p \to p + X)/\sigma(pp \to p + X)$ is a function of $x_T$ and $\theta$ only. This ratio is a good test of the leading-particle model, since at $\theta = \pi/2$ it is not sensitive to the quark-proton cross section. On the other hand, the angular dependence of this same ratio is very sensitive to the $q$-$p$ cross section. We can thus test with the beam ratio two different aspects of the leading-particle model; at $\theta = \pi/2$ it is a test of the model itself and of the particular choices we made for the structure functions and $g_p(z)$, while the angular dependence of the ratio tests the angular dependence of the $q$-$p$ scattering.

Figure 13 shows our result for the beam ratio at $\theta = \pi/2$. This result can be simply understood in terms of the ratio between the pion and proton quark distributions. As we saw in Fig. 12, $\langle x \rangle$, the average longitudinal fraction of the momentum carried by the quarks, increases almost linearly with $x_T$ and therefore we obtain an increasing $\pi/p$ beam ratio as $x_T$ increases, since the quark distribution for the pion behaves like $(1 - x)$ at large $x$, as compared to $(1 - x)^4$ for the proton (Table I). At very small $x_T$ ($x_T \ll 0.1$) the beam ratio ap-

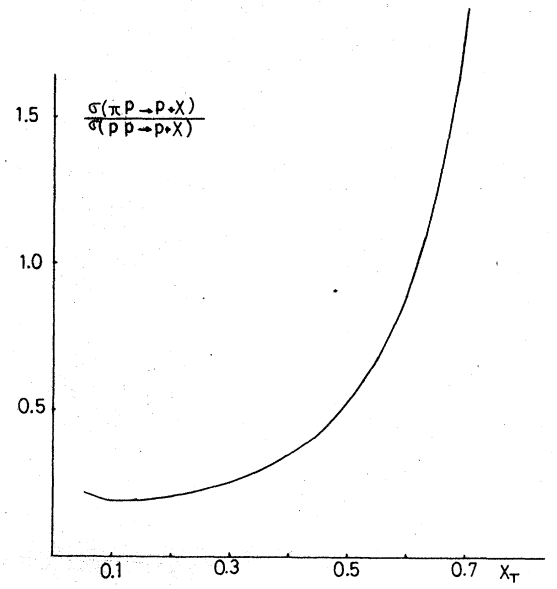


FIG. 13. The beam ratio $\sigma(\pi p \to p+X)/\sigma(pp \to p+X)$ as a function of $x_T$ at $\theta=\pi/2$.

proaches $\frac{1}{3}$, which is equal to the ratio between the correspondent sea distributions ($\frac{2}{3}$) divided by 2; as with a pion beam the large-$p_T$ proton can only come from the target, while with a proton beam it could come from either the beam or the target.

The angular dependence of the $\pi/p$ beam ratio is more complicated as it is very sensitive to the angular dependence of the quark-proton scattering, while, of course, being still dependent on the quark distributions. It is the interplay of these two factors which determines the actual variation with angle of the beam ratio.

There are two important clues for the understanding of the results displayed in Figs. 14(a) and 14(b), where we show the beam ratio at two angles ($\theta=45°$ and $\theta=135°$) and for two choices of the function $\psi$. The first is that in $pp \to p+X$ there are two contributions to the leading-particle process of Fig. 8, one in which the quark comes from the beam and the second one in which it comes from the target, while in $\pi p \to p+X$ the quark can only come from the pion beam. It so happens that as the c.m. angle decreases at fixed $x_T$, the average longitudinal fraction $\langle x \rangle$ of the momentum carried by the quark coming from the beam particle increases. Therefore, owing to the behavior of the quark distributions, we expect that as the c.m. angle decreases at fixed $x_T$, the $\pi/p$ beam ratio increases, as shown in Fig. 14(a). On the other

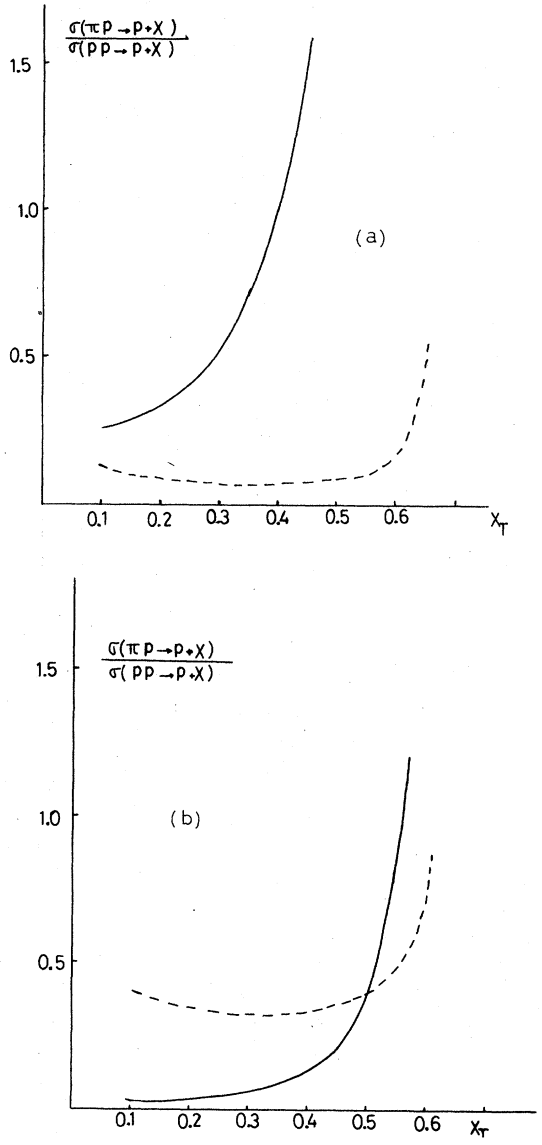


FIG. 14. (a) Angular dependence of the $\pi/p$ beam ratio when $|\psi|^2=\hat{s}^6/\hat{u}^6$. Solid line is for $\theta=45°$ and the dashed one is for $\theta=135°$.

hand, $\pi p \to p+X$ is not symmetrical as $\theta \to \pi-\theta$, while $pp \to p+X$ is. Consequently if the angular behavior of the $q$-$p$ scattering (the function $\psi$) is such as to give a $pp \to p+X$ cross section which is peaked at forward angles, then $\pi p \to p+X$ will tend to be peaked at backward angles. Therefore, at intermediate $x_T$ the $\pi/p$ beam ratio will be greater backwards than forwards, as seen in Fig. 14(b). However, as $x_T$ increases approaching its kinematical limit, the first effect due to the quark distribution tends to overcome the second one, ex-

plaining why at large $x_T$ the beam ratio at 45° is greater than at 135° [Fig. 14(b)].

### B. The jet cross section

We can ask: What is the cross section for the production of a large-$p_T$ baryon jet unconstrained by the requirement of having a single large-$p_T$ proton? We expect it to be two orders of magnitude larger than the single proton cross section, simply on the grounds of the trigger bias effect.[25] That this is indeed so can be seen in Fig. 15 where we have plotted the ratio $\sigma(pp \to \text{baryon jet} + X)/\sigma(pp \to p + X)$ at $\theta = \pi/2$, as a function of $x_T$. We find that at $x_T = 0.4$ this ratio is about 200 and that it increases to about $10^3$ at $x_T = 0.7$.

As protons constitute a significant fraction of the single-particle yield at high $p_T$ ($\approx 30\%$) we therefore expect that the calorimeter experiments[27] which trigger on jets will contain an appreciable number of baryons ($\approx 10\%$).

### C. Away-side rapidity distribution

It has been known since its proposal[10] that the leading-particle model has a very peculiar event structure. In particular, triggering on a proton which has been produced alone with a given $p_T$ and rapidity $y$, the away-side quark is scattered at a fixed and narrow angle to the beams. The away-side rapidity distribution has therefore a sharp peak at this value of the rapidity. Simple kinematics shows that the rapidity of the away-side quark is given by

$$y' = \ln\left(\frac{2}{x_T} - e^{y}\right). \tag{37}$$

Thus, for example, with $y = 0$ and $x_T = 0.2$, the away-side distribution will have a peak at $y = 2.2$ ($\theta' \approx 13°\%$), which is indeed a very narrow angle with respect to the beams.

Notice that as we move the trigger forward, the away-side system slightly moves backward.

Introducing a jet on the same side of the proton trigger, as done in Sec. III C through the jet fragmentation function $g_p(z)$ [see Eq. (29)], modifies these results slightly as now the away-side system does not have necessarily to come out at a definite angle but its rapidity can vary from event to event. Even so, the rapidity distribution is still peaked at small angles, and in particular we notice that if the trigger is at $\theta = \pi/2$ ($y = 0$), the rapidity distribution $dN/dy'$ vanishes for $y' = 0$ ($\theta' = \pi/2$), which is a very striking signature of the model.

We show in Fig. 16 the away-side rapidity distribution assuming that the away-side quark fragmentation function behaves like $(1-z)^2$ near $z = 1$, as indicated by the recent data from DASP[28] and PLUTO,[29] at DESY. The normalization in Fig. 16 is arbitrary as we are more interested in the shape of the distribution and as our calculation is not completely realistic, having neglected smearing, effects due to the parton transverse momentum and the transverse-momentum spread of the jet's fragments[19,20] which is likely to alter both the

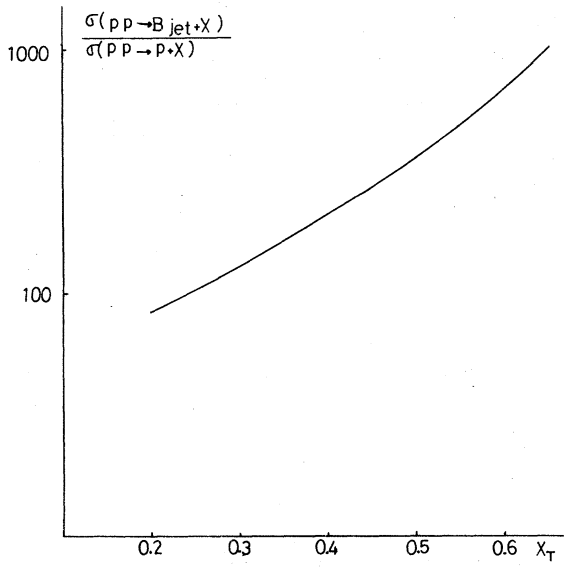


FIG. 15. The ratio between the baryon jet and the single-proton cross sections, $\sigma(pp \to \text{baryon jet} + X)/\sigma(pp \to p + X)$.

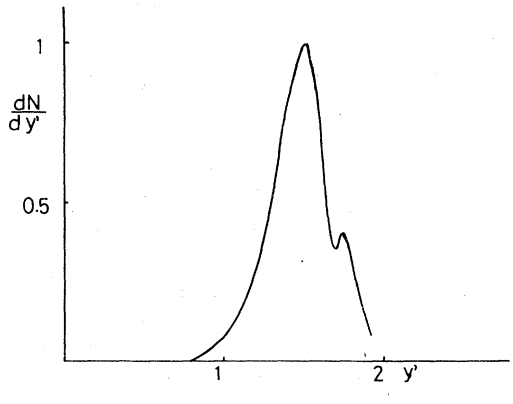


FIG. 16. The away-side rapidity distribution in the leading-particle model. The normalization is arbitrary and the curve is calculated for $x_T = 0.2$, $\sqrt{s} = 23$ GeV. The away-side quark has $2.5 < p_T < 1.5$ GeV.

shape (smearing the forward peak) and the normalization of $dN/dy'$.

The small peak in Fig. 16 is due to the smeared (because of finite experimental resolution) $\delta$ function corresponding to the single-particle term in the jet fragmentation function (29). The relative size of the two peaks in $dN/dy'$ is determined by the ratio between $b_p$ and $a_p$ in (29), and the smallness of the second peak reflects the smallness of $b_p$ as compared to $a_p$.

In Fig. 17 we show how the position of the maximum of $dN/dy'$ changes as we vary the rapidity of the trigger, for a fixed value of $x_T$. We still notice a tendency of the away-side system to move backward as the trigger is moved forward. Notice the small angles at which the away-side quark emerges.

With pion beams, as the large-$p_T$ proton comes from the target, the rapidity distribution on the away-side is not symmetrical around $y'=0$, unlike the case for proton beams. Consequently $dN/dy'$ will have a peak at very large angles. All the above results are qualitatively unchanged for pion beams, with the proviso that we replace $y'$ by $-y'$ when changing from proton to pion beams.

### D. Associated multiplicities

We have discussed previously (see Sec. II D) the question of the multiplicities associated with a large-$p_T$ proton in the framework of the multiple-scattering model. Use was made in that discussion of the DILR data.[17] We here discuss again this problem, but now using the leading-particle model and paying more attention to the same-side multiplicity.

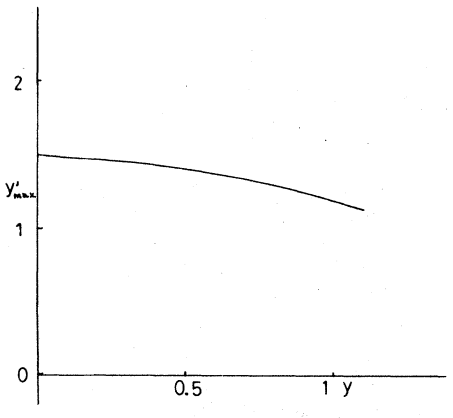


FIG. 17. Variation of the position of the maximum of the away-side rapidity distribution, as the trigger rapidity changes. The trigger has $x_T=0.3$.

In a very approximate way, neglecting the longitudinal components of the momentum and the transverse width of the jet, the momentum carried by the fragments of the same-side jet, excluding the trigger itself, is given by

$$P=\frac{1-\langle z\rangle}{\langle z\rangle}P_T^{\text{trigger}} \tag{38}$$

where $\langle z\rangle$ is the average fraction of the jet's momentum which is carried by the trigger.

Assuming, as we did before, that the multiplicity is logarithmic on the momentum of the fragmenting system, the same-side multiplicity is given by

$$\langle n_h\rangle=a_h+b_h\ln\left[\frac{(1-\langle z\rangle_h)}{\langle z\rangle_h}P_T^{\text{trigger}}\right], \tag{39}$$

where the subscript $h$ denotes the trigger type.

It is clear that in the simple leading-particle model, where the trigger is produced alone and therefore $\langle z\rangle_p=1$, we of course obtain $\langle n_p\rangle<\langle n_\pi\rangle$. Introducing the same-side jet in the leading-particle model will obviously improve this result. As we have seen in Fig. 12(a), $\langle z\rangle_p=0.75$ at $x_T\approx 0.2$ and this will have the consequence of substantially increasing the same-side multiplicity. For the sake of comparison, we calculate the proton minus pion trigger same-side multiplicities at $p_T=3\text{GeV}/c$ and $\sqrt{s}=45$ GeV. Using for convenience $\langle z\rangle_\pi=0.82$ as we did before (see Sec. II D), we obtain

$$\langle n_p\rangle-\langle n\rangle_\pi=0.25,$$

which agrees with the experimental value.[17]

Turning now to the away-side multiplicity, we notice that in the case of the leading-particle model, it is wrong to neglect the longitudinal component of the momentum of the away-side quark, an approximation made by some authors.[11] As we have seen in (4.3), the away-side quark is emitted at a very narrow angle and has therefore a very large longitudinal momentum. What is more, comparison with the DILR data is meaningless, as their experiment covers a range of rapidity, $|y'|<1.5$, while in the leading-particle process, as can be seen from (37) and Fig. 17, the away-side quark has $y'\approx 2.5$ (for $x_T\approx 0.15$), which is well outside the DILR range.

### E. General picture of the event structure in the leading-particle model

We have seen in Sec. IV C that the away-side rapidity distribution in the leading-particle model is very different from that obtained in other large-$p_T$ models. In this section we comment on other features of the event structure which help to distinguish the leading particle from other models.

The first aspect concerns the background of low-$p_T$ particles, typical of ordinary hadronic collisions, which is observed to underlie a large-$p_T$ reaction.[5]

In conventional hard-scattering models, with the diagrammatic structure of Fig. 18, it has been shown by DeTar, Ellis, and Landshoff[7] that initial- and final-state interactions do not contribute to the leading asymptotic behavior of the single-particle inclusive cross section but do have an important effect on the structure of the final states, contributing to the low-$p_T$ background mentioned above. In particular, they showed that the states reached by pionization scale with energy in the same way as the large-$p_T$ process.

These results are, however, not true (in conventional parton models[30]) for diagrams with the structure of the handbag diagram of deep-inelastic leptoproduction (Fig. 19), where the contribution from final states with pionization decreases more rapidly with energy than the contribution without final state interactions, i.e., the simple handbag diagram.[7,31] It so happens that the leading-particle model has exactly the same diagrammatic structure as the handbag diagram of leptoproduction and consequently this result holds true for it as well. We therefore expect that in the leading-particle model the low-$p_T$ background will be smaller than in other large-$p_T$ models and hope that this effect may be amenable to experimental observation.

Our second remark has to do with the correlation between a large-$p_T$ particle and a fast forward moving positive particle (leading particle). Recently the BFS collaboration[32] studied this problem using different types of triggers and found that the correlation shows a dependence on trigger species. The most noticeable difference is observed when the trigger is a large-$p_T$ proton in which case there are significantly fewer associated fast forward moving positive particles than in the case of other triggers. This is seen in Table II with the data from Ref. 32 showing the number of forward particles with $x_{\parallel}=2p_{\parallel}/\sqrt{s}>0.4$ associated with a trigger of type $A$ relative to a trigger of type $B$ (averaged over all $p_T>$ GeV).

The leading-particle model gives a natural explanation for this result as in this mechanism the large-$p_T$ proton is removed from the beam and is scattered at high $p_T$ into the central region, thus decreasing the number of forward moving protons. (Notice that the multiple-scattering model also predicts a much smaller number of leading particles when triggering on a large-$p_T$ proton, as now all three valence quarks of both colliding protons are scattered into the central region. We suspect that the suppression of the leading-particle effect is even more pronounced in the multiple-scattering model.)

We do not attempt in this paper to compute quan-

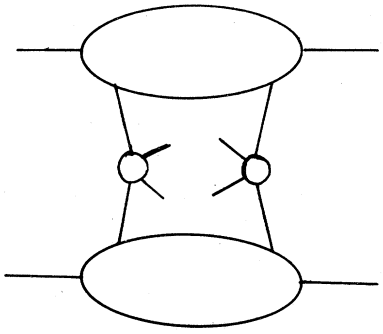

FIG. 18. Basic diagram for hard-scattering models of large-$p_T$ production.

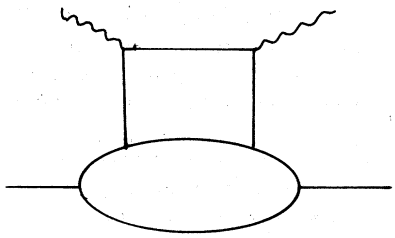

FIG. 19. The handbag diagram for leptoproduction.

TABLE II. Number ($N_A$) of forward positive particles ($|x_{\parallel}|>0.4$) associated with a trigger of type $A$ relative to a trigger of type $B(N_B)$ averaged over all $p_T^{\text{trigger}}>1$ GeV/$c$.

| $A/B$ | $N_A/N_B$ |
|---|---|
| $\pi^+/\pi^-$ | $0.92\pm0.02$ |
| $K^+/\pi^+$ | $1.00\pm0.02$ |
| $p/\pi^+$ | $0.83\pm0.03$ |
| $K^-/\pi^-$ | $0.95\pm0.03$ |
| $\bar{p}/\pi^-$ | $0.91\pm0.03$ |

titatively this effect but remark that the data can be qualitatively understood if a significant number of the high-$p_T$ protons are produced by a leading-particle process such as the one described in this paper.

To conclude, we stress that the experimental study of the final states accompanying a large-$p_T$ proton is the best ground for testing the leading-particle model. Also, as mentioned in Sec. IV A, the production of large-$p_T$ protons by a pion beam would enable us to test this model in a very neat way.

*Note added.* In Sec. II F we remarked that the transverse momentum of the quarks inside the hadrons is probably not negligible in single-scattering models. It should be stressed that this view is not unique, evidence to the contrary being provided in Refs. 33–35.


## ACKNOWLEDGMENTS

I would like to thank Dr. P. V. Landshoff and Professor J. C. Polkinghorne for their constant interest in this work and for many useful suggestions. I acknowledge the financial support given by the British Council.


---

*Present address: Instituto de Fisica Teórica, Rua Pamplona 145-01405, São Paulo, Brazil.


[1]J. W. Cronin *et al.*, Phys. Rev. D 11, 3105 (1975).

[2]D. Antreasyan *et al.*, Phys. Rev. Lett. 38, 115 (1977).

[3]B. Alper *et al.*, Nucl. Phys. B100, 237 (1975).

[4]R. D. Field and R. P. Feynman, Phys. Rev. D 15, 2590 (1977).

[5]P. Darriulat, in *Proceedings of the XVIII International Conference on High Energy Physics, Tbilisi, 1976,* edited by N. N. Bogolubov *et al.* (JINR, Dubna, U. S. S. R., 1977), Vol. I, p. 14–23.

[6]L. Kluberg *et al.*, Phys. Rev. Lett. 38, 670 (1977).

[7]C. DeTar, S. D. Ellis, and P. V. Landshoff, Nucl. Phys. B87, 176 (1975).

[8]P. V. Landshoff, J. C. Polkinghorne, and D. M. Scott, Phys. Rev. D 12, 3738 (1975), hereafter referred to as LPS.

[9]P. V. Landshoff, Phys. Rev. D 10, 1024 (1974).

[10]P. V. Landshoff and J. C. Polkinghorne, Phys. Rev. D 10, 891 (1974); D. M. Scott, Nucl. Phys. B74, 524 (1974).

[11]G. C. Fox, in *Particles and Fields '76,* proceedings of the Annual Meeting of the Division of Particles and Fields of the APS, edited by H. Gordon and R. F. Peierls (BNL, Upton, New York, 1977), p. G1.

[12]S. J. Brodsky and G. Farrar, Phys. Rev. Lett. 31, 1153 (1973); V. Matveev *et al.*, Lett. Nuovo Cimento 7, 719 (1973).

[13]J. D. Bjorken and J. Kogut, Phys. Rev. D 8, 1341 (1973); D. M. Scott, Nucl. Phys. B74, 524 (1974).

[14]A. Donnachie and P. V. Landshoff, Nucl. Phys. B112, 233 (1976).

[15]S. Pokorski and L. Van Hove, Nucl. Phys. B86, 243 (1975); L. Van Hove, Acta Phys. Pol. B7, 339 (1976).

[16]See R. Cutler and D. Sivers, Phys. Rev. D 16, 679 (1977) and references therein.

[17]B. Alper *et al.*, Nucl. Phys. B111, 1 (1976).

[18]W. Morton, Nucl. Phys. B119, 461 (1977).

[19]P. V. Landshoff, Cambridge Report No. DAMTP 77/28 (unpublished).

[20]M. Della Negra, in *Proceedings of the 1977 European Conference on Particle Physics, Budapest,* edited by L. Jenik and I. Nontvay (CRIP, Budapest, 1978).

[21]Note added in proof, Ref. 8.

[22]P. V. Landshoff and J. C. Polkinghorne, Phys. Rev. D 18, 3344 (1978).

[23]H. Bøggild, in Proceedings of the VIII International Colloquium on Multiparticle Reactions, Kayserberg, 1977 (unpublished).

[24]D. Sivers, S. Brodsky, and R. Blankenbecler, Phys. Report C23, 1 (1976).

[25]S. D. Ellis, M. Jacob, and P. V. Landshoff, Nucl. Phys. B108, 93 (1976).

[26]M. Della Negra *et al.*, Nucl. Phys. B127, 1 (1977).

[27]C. Bromberg *et al.*, Phys. Rev. Lett. 38, 1447 (1977).

[28]DASY collaboration: R. Brandelik *et al.*, Phys. Lett. 67B, 358 (1977).

[29]PLUTO collaboration: G. Knies, in *Proceedings of the International Symposium on Lepton and Photon Interactions at High Energies, Hamburg, 1977,* edited by F. Gutbrod (DESY, Hamburg, 1977).

[30]P. V. Landshoff and J. C. Polkinghorne, Nucl. Phys. 5C, 1 (1972).

[31]P. V. Landshoff and J. C. Polkinghorne, Nucl. Phys. B33, 221 (1971).

[32]M. Albrow *et al.*, Nucl. Phys. B135, 461 (1978).

[33]W. Caswell, R. Horgan, and S. J. Brodsky, Phys. Rev. D 18, 2415 (1978).

[34]F. Halzen, G. A. Ringland, and R. G. Roberts, Phys. Rev. Lett. 40, 991 (1978).

[35]K. Kinoshita and Y. Kinoshita, Report No. KY USHU-78-HE-6, 1978 (unpublished).